J Mater Sci (2016) 51:937–949
DOI 10.1007/s10853-015-9423-0

Preparation and evaluation of Fe_3O_4 nanoparticles incorporated molecularly imprinted polymers for protein separation

Shu Yang[1] · Xin Zhang[1] · Wentao Zhao[1] · Liquan Sun[1] · Aiqin Luo[1]

Received: 21 May 2015 / Accepted: 8 September 2015 / Published online: 18 September 2015

Abstract Protein imprinting is still a challenge due to the low binding kinetics and poor binding selectivity. In this study, a facile method of the preparation of magnetic molecularly imprinted polymers (MIPs) for selective protein separation was reported. Carboxyl group functionalized Fe_3O_4 nanoparticles (NPs) were synthesized using a solvothermal method. After pre-assembly of caroxyl group functionalized Fe_3O_4 NPs and template protein lysozyme (Lyz) to form Lyz–Fe_3O_4 complex, magnetic MIPs were synthesized by a sol–gel process of 3-aminopropyltriethoxylsilane and tetraethyl silicate with Lyz–Fe_3O_4 complex incorporated. Then Fe_3O_4–MIPs particles with magnetic response could be collected by simple crush of bulk polymers. This preparation process avoid the need of high dilution of monomer for anti-agglomeration in the surface imprinting, and large amount of solvent is spared. The morphology and structure property of the prepared magnetic NPs were characterized by transmission electronic microscopy, Fourier transform infrared spectroscopy, and vibrating sample magnetometer. Binding experiments were carried out to evaluate Fe_3O_4–MIPs particles' binding performance and selectivity. And results showed fast binding kinetics, high binding capacity, and favorable specific recognition behavior toward template protein, which is due to the role of carboxyl group functionalized Fe_3O_4 NPs as both magnetic source and importantly as co-functional monomer incorporated in the polysiloxane imprinting system. Real egg white sample tests demonstrate good separation effect. This report provides a possibility of the selective separation of protein in complex matrix.

✉ Aiqin Luo
aqluobit@163.com

[1] School of Life, Beijing Institute of Technology, No. 5 Zhongguancun South Street, Haidian District, Beijing 100081, People's Republic of China

Introduction

Molecular imprinting has been widely recognized as a promising technique for constructing synthetic polymers with selective recognition cavities that are complementary in shape, size, and functionality with respect to the template molecules [1]. For the past few decades, the interest and attention shown toward this field have been increasing at an amazing pace. With the merits of mechanical and chemical stability, ease of preparation, wide range of operating conditions, and high specificity, the potential applications of molecularly imprinted polymers (MIPs) cover a wide range of separation, catalysis, analytical chemistry, and biosensing [2, 3]. And MIPs have been successfully applied to the recognition of small molecules [4–12].

However, relatively little progress has been made in the area of protein imprinting due to the influence of large size, complexity, conformational flexibility, and solubility of proteins [1]. The imprinting of proteins into polysiloxane or polyacrylamide polymers in buffer solutions has suffered from unsatisfactory binding kinetics, low binding capacity, low specificity, and reproducibility. To address these problems, surface imprinting onto supporters [13–20] and epitope imprinting with a fragment of the original protein as template [21, 22] have been developed. For epitope imprinting, finding the proper epitope on the target protein surface is time- and cost-consuming; thus only a few work has been presented. Surface imprinting can somewhat overcome the template transfer difficulty to

achieve better binding kinetics, thus seems to dominate the protein imprinting [23]. But surface imprinting of protein is still hindered by the low binding capacity and relatively low binding specificity [24–26]. Furthermore, in the process of surface imprinting of protein, low concentration monomers are involved to avoid the possible gelation of the dispersion and to get the unagglomerated imprinted particles [24], but the gelation reduction is limited and a large amount of solvent is needed. And for practical usage the separation of nano MIPs is another problem.

Recently, recognition materials combining magnetic nanotechnology with molecular imprinting have been attracting more and more attention. MIPs with magnetic response can be easily separated from complicated samples by the aid of an external magnet without any pretreatment such as centrifugation and filtration. And as magnetic nano cores have small size, large surface-to-volume ratio, and well-defined material shape, surface coating with a thin imprinted polymer shell is expected to improve MIP's binding kinetics, binding capacity, and binding site accessibility with more complete removal of templates and lower mass transfer resistance [15].

For surface imprinting, Fe_3O_4 nanoparticles (NPs) are the commonly employed magnetic core which can be modified by silane [19] or other active groups (such as vinyl [27], carboxyl [26], aldehyde [28], boronic acid [29], Cu^{2+}-iminodiacetic acid group [30], and functional initiator for controlled/"living" polymerization [17, 31]) through one or more steps. Although through fine synthesis methods the core–shell structure functionalized magnetic nanospheres with a thin coating can get improved binding kinetics and binding capacity, still some tricks are needed to further control successful imprinting shell formation and to improve the binding capacity and specificity for practical usage. And surface imprinting of protein is currently undergoing extensively study.

On the other side, molecular imprinting with bulk polymerization is more straightforward and effective. A few papers had been published about the imprinting of bovine serum albumin (BSA) [32], lysozyme (Lyz) [33, 34], bovine hemoglobin (BHb) [35], and other proteins [36–41] that employing bulk polymerization method. Bulk polymerization for protein imprinting was not favorable in the past, for it was considered to be with the drawbacks of low binding kinetics and difficult template removal, and not suitable for chromatography [42–44]. But with the merits of higher binding capacity, higher binding specificity, and easier preparation, protein imprinting with bulk polymerization can be a good choice for selective separation or other kind of application than chromatography. And the combination of bulk polymerization of molecular imprinting and magnetic separation would ideally provide a powerful analytical method with remarkable characteristics of selectivity, simplicity, and flexibility.

In this work, carboxyl group functionalized Fe_3O_4 NPs were synthesized using a one-pot hydrothermal method, and used as both co-functional monomer and magnetic source to prepare magnetic MIPs for protein separation. The carboxyl group as co-functional monomer was incorporated in the polysiloxane imprinting system to provide more non-covalent binding sites. The non-covalent interaction between target protein and MIPs facilitates template removal and fast binding kinetics. And the preparation process is direct and simple. The binding kinetics, binding capacity, binding selectivity, and binding specificity of the obtained polymers were evaluated. Furthermore, the practicability for biological application was further investigated by specific separation of the template protein from standard binary and ternary protein mixture and real egg white sample. Results demonstrate a good prospect for real application.

Experiments and methods

Chemicals

Lysozyme (Lyz, pI 11.2, MW 14.4 kDa), bovine serum albumin (BSA, pI 4.9, MW 66.0 kDa), and ovalbumin (OVA, pI 4.7, MW 43.0 kDa) were purchased from Hess Leber Biotechnology Co. Ltd. Beijing. Bovine hemoglobin (BHb, pI 6.9, MW 64.5 kDa) was purchased from Sigma-Aldrich (Beijing, China). Tetraethyl silicate (TEOS) and ethylene glycol (EG) were purchased from Xilong chemistry Co. Ltd. (Shantou, China). 3-aminopropyltriethoxyl silane (APTES) were purchased from Beijing J&K Chemical Technology Co. Ltd. (Beijing, China). Ferric chloride crystal ($FeCl_3 \cdot 6H_2O$) was purchased from Tianjin Fuchen Chemical Reagents Works (Tianjin, China). Anhydrous sodium acetate (NaAc) and Trisodium citrate dihydrate ($Na_3Cit \cdot 2H_2O$) were provided by Beijing Chemicals Ltd. (Beijing, China). The egg white sample was collected from fresh egg from the local market. HPLC grade acetonitrile was obtained from Beijing J&K Chemical Technology Co. Ltd. (Beijing, China). All other reagents used were of AR grade and used as received without further purification. Doubly distilled (D.D.) water was used in this work.

Instruments

The structures and morphologies of the materials were examined using transmission electronic microscopy (TEM, Hitachi H-800, Japan). Fourier transform infrared (FT-IR)

spectra (4000–400 cm^{-1}) in KBr were recorded on a Spectrum BX spectrophotometer (PerkinElmer, USA). Protein adsorption data were recorded on a UV-1800 UV–Vis spectrophotometer (Shimadzu, Japan). Room temperature magnetization isotherms of magnetic nanospheres were obtained using a vibrating sample magnetometer (VSM, Lake Shore 7307, US). PowerPac Basic apparatus (Bio-Rad, Hercules, CA) was used for SDS-PAGE analysis. All chromatographic measurements were performed by Waters ACQUITY UPLC H-Class (USA) and a Tosoh TSKgel C4-300 (150 mm × 4.6 mm, 3 μm, 300 Å) column (Japan). In addition, a drying oven on forced convection(Shanghai Keelrein instrument Co. Ltd, China), an incubator shaker THZ-D (Huamei Biochemistry, Jiangsu, China), and a vacuum drying oven DZF-6020 (Shanghai Yiheng Technical Co., LTD, China) were also used in the experiments.

Synthesis of carboxyl-functionalized Fe_3O_4 NPs

The carboxyl-modification Fe_3O_4 NPs (denoted as Fe_3O_4@COOH) were synthesized according to a previous report [45] with some modifications. Briefly, $FeCl_3{\cdot}6H_2O$ (0.65 g), NaAc (1.2 g), and $Na_3Cit{\cdot}2H_2O$ (0.2 g) were dissolved in EG (20 mL) under persistent stirring until a homogeneous yellow solution was obtained and transferred into the Teflon-lined stainless-steel autoclave. The solution was sealed and heated at 200°C for 10 h. The resultant black products were washed with D.D. water and ethanol to remove the solvent and unreacted reagents, and then dried in vacuum for further use.

Preparation of MIPs incorporated with Fe_3O_4 NPs

TEOS activation solution was first prepared. Briefly, TEOS (6.6 mL) was added into the mixture of 0.1 M HCl (1.6 mL), D.D. water (1.2 mL), and ethanol (2 mL), standing still for 24 h at room temperature. Lyz (10 mg) was dissolved in 10 mM PB buffer (pH 7.0, 10 mL) in a beaker, and mixed with Fe_3O_4@COOH NPs (20 mg), then APTES (990 μL) were added and mechanically stirred for 3 h at room temperature. Then TEOS activation solution was added into the above mixture for polymerization. After that, the product was left standing for another 12 h, then put in the drying oven overnight at 40 °C. The obtained products were ground, then rinsed with D.D. water and separated by external magnet for three cycles. Then 10 % (v/v) acetic acid 10 % (w/v) SDS solution as eluent was added to remove the template protein until no Lyz in the supernatant was detected with a UV/Vis spectrophotometer at 280 nm wavelength. The resulting imprinted polymers (denoted as Fe_3O_4–MIPs) were collected by an external magnet and washed with D.D. water, then dried under vacuum. Non-imprinted Fe_3O_4–NIPs were prepared following the same procedure in the absence of the template protein Lyz.

Binding experiments

Binding kinetics

Binding kinetics was tested by changing the adsorption time at regular intervals from 5 to 45 min while adopting the same initial concentration of Lyz at 3.0 mg mL^{-1}.

The adsorption capacity (Q) of the template protein or competitive protein bound to the imprinted polymers is defined as

$$Q = \frac{(C_0 - C_e)V}{W} \quad (1)$$

where C_0 and C_e (mg mL^{-1}) are the initial concentration and the free analytical concentration of the template protein or competitive protein at equilibrium, V (mL) is the volume of the initial solution, and W (g) is the weight of the imprinted polymers. The binding tests were performed thrice in parallel.

Binding isotherms

Binding isotherms were achieved by batch binding tests, experiment was carried out through changing the concentrations of Lyz from 0.05 to 5.0 mg mL^{-1} while employing the same adsorption time of 30 min. And the binding capacity was calculated as above.

Binding selectivity

The binding selectivity of the Fe_3O_4–MIPs and Fe_3O_4–NIPs was studied using OVA, BSA, and BHb as comparative proteins with concentrations of 1.0 mg mL^{-1}. The concentration of comparative proteins was measured by UV/Vis spectrometry at the wavelength of 280 nm for BSA and OVA, and wavelength of 406 nm for BHb.

The imprinting factor (IF) and selectivity coefficient (SC) are used to evaluate the selectivity properties of Fe_3O_4–MIPs and Fe_3O_4–NIPs toward the template protein and competitive protein. The IF and SC are calculated from the following equations:

$$IF = \frac{Q_{MIP}}{Q_{NIP}} \quad (2)$$

$$SC = \frac{IF_{TEM}}{IF_{COM}} \quad (3)$$

where Q_{MIP} and Q_{MIP} (mg g^{-1}) represent the adsorption capacity of proteins for Fe_3O_4–MIPs and Fe_3O_4–NIPs, IF_{TEM} and IF_{COM} are the IFs for template protein and competitive protein.

Competitive binding test

Competitive binding tests were verified by using the mixed solution. The separation of binary and ternary protein mixture were carried out. 10 mg Fe_3O_4–MIPs or Fe_3O_4–NIPs were subjected to the binary protein mixture solution of BSA (1.0 mg mL^{-1}) and Lyz (1.0 mg mL^{-1}), and ternary protein solution of BSA (1.2 mg mL^{-1}), OVA (1.2 mg mL^{-1}) and Lyz (1.2 mg mL^{-1}), respectively. The adsorption experiments were carried out in a same manner as mentioned above. The concentration of each protein in the mixture solutions was determined using HPLC method.

Real sample separation

15 mg of Fe_3O_4–MIPs was merged with 4 mL of diluted egg white (chicken egg white sample diluted 40-fold with PB buffer solution, pH 7.0, 10 mM). After incubation for 30 min under gentle shaking, the Fe_3O_4–MIPs were separated by an external magnet and eluted with 10 % (v/v) acetic acid 10 % (w/v) SDS solution for 30 min to remove the absorbed protein. The diluted, absorbed, and eluted samples were analyzed with SDS-PAGE. To further quantitatively confirm the separation result, HPLC analysis was employed for diluted and absorbed sample.

Characterization

The morphology and structure of Fe_3O_4 NPs and Fe_3O_4–MIPs were examined by a Hitachi transmission electron microscope (TEM, Hitachi H-800, Japan). FT-IR analysis was recorded using the Spectrum BX spectrophotometer (PerkinElmer, USA). The magnetic properties were analyzed with VSM (VSM, Lake Shore 7307, US). The concentration of single protein solution was obtained by using a UV-1800 spectrophotometer (Shimadzu, Japan). Electrophoretic analysis of protein samples was performed using PowerPac Basic (Bio-Rad, Hercules, CA) with 15 % running and 5 % stacking gels. Proteins were stained with Coomasie Brilliant Blue R-250. HPLC analysis of protein samples was performed on Waters ACQUITY UPLC H-Class system (USA) with a Tosoh TSKgel C4-300 (150 mm × 4.6 mm, 3 μm, 300 Å) column (Japan). Gradient elution program was as follows: solution A: 10 vol% acetonitrile and 90 vol% D.I. water with 0.05 vol% trifluoroacetic acid (TFA), solution B: 80 vol% acetonitrile and 20 vol% D.I. water with 0.05 vol% TFA. Linear gradient for competitive binding tests is from 65 to 10 % A in 10 min, and for real chicken white sample is from 100 to 0 % A in 35 min, with UV detection wavelength at 280 nm, flow rate 0.8 mL min^{-1} and injection volume 10 μL.

Results and discussion

Preparation of magnetic imprinted polymers

The scheme for the synthesis of Fe_3O_4–MIPs is illustrated in Fig. 1. First, functionalized Fe_3O_4@COOH NPs were prepared with a modified one step solvothermal method, and whose surface were coated with carboxyl groups. Next, template protein Lyz was immobilized on the surface of Fe_3O_4@COOH NPs to form template-Fe_3O_4 complex through hydrogen bond and electrostatic interaction between the carboxyl groups on the exterior of Fe_3O_4@COOH NPs and amino or carboxyl groups of the proteins. Then, APTES-TEOS siloxane co-polymerization with the Lyz–Fe_3O_4 complex resulted in a polymeric network that molded around template-Fe_3O_4 complex. And numerous non-covalent interaction could be formed between Lyz–Fe_3O_4 complex and the silanol groups of the polysiloxane, the amino groups of APTES and the alkyl chains of TEOS. The Fe_3O_4 NPs were incorporated into this imprinted polymer network, providing multiple functions with binding site for target protein recognition and magnetic response property. And MIPs particles can be easily got by further grinding. Finally, after the removal of the template proteins with 10 % (v/v) acetic acid 10 % (w/v) SDS solution, MIPs with imprinted cavities complementary to Lyz in shape, size, and functional group orientation was obtained.

Compared with those previous reported surface imprinting methods for protein recognition using Fe_3O_4 NPs as supporters, the process of this preparation method was more straightforward, time-saving, and cost-effective. First, the synthesis of carboxyl group functionalized Fe_3O_4 NPs only took one step in this paper, which avoid the relatively complicated multi-step modifications of Fe_3O_4 NPs as evidenced in articles [1, 16, 24, 27, 28, 31, 46–49]. Second, after immobilization of protein, APTES-TEOS monomer imprinting system with sol–gel process for bulk polymerization is economic and effective. Often solvent is heavily employed for surface imprinting with highly diluted monomer concentration [24, 25], but agglomeration still existed [46]. For bulk polymerization large amount of solvent is spared. Later experimental results showed that this method could get better imprinting effect. And compared with MIPs prepared by conventional bulk polymerization, Fe_3O_4–MIPs prepared in this paper demonstrated an improved binding kinetics with high binding specificity and easy usage. This work displayed some advantages in the aspect of preparation technology.

The carboxyl-functionalized Fe_3O_4 NPs incorporated in the polysiloxane play an important role for protein recognition, as carboxyl functional group in the imprinted

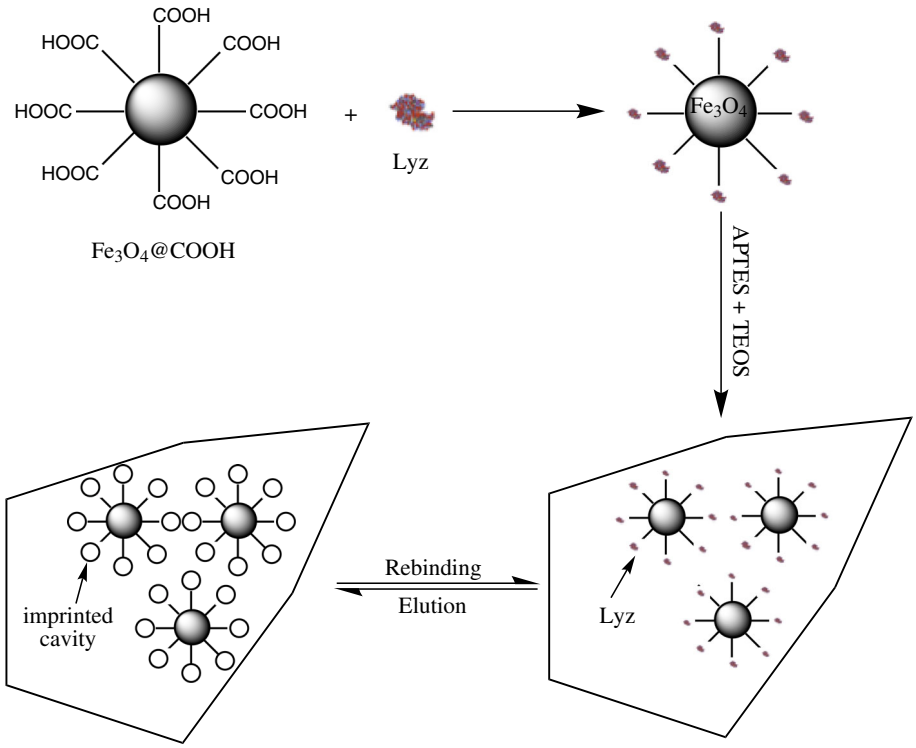

Fig. 1 Schematic illustration of Fe_3O_4–MIPs preparation

polymer network can provide more kinds of binding interactions for protein imprinting, thus improve the binding capacity and binding specificity. It was evidenced that methacrylic acid (MAA) as functional co-monomer can provide electrostatic interaction with protein, thus improving the imprinting effect in the acrylamide (AAm) - *N*,*N*′-methylenebisacrylamide (MBA) imprinting combination [25, 33]. Some work about protein imprinting also adopted MAA or other carboxyl-monomer as functional co-monomer [27, 46, 48]. APTES-TEOS (or octyltrimethoxysilane, OTMS) bifunctional monomers combination for sol–gel process imprinting are commonly employed, with longer hydrophobic alkyl chain for limited improvement of protein imprinting [15, 28, 49]. But to the best of our knowledge, there is no report about carboxyl group functional monomer incorporated into this imprinting combination. In this work, Fe_3O_4@COOH NPs was incorporated into the imprinted polymer network, which act with two effect: one as magnetic response material, the other as functional co-monomer to provide carboxyl group for protein binding. And an improved imprinting effect for protein recognition is expected.

Also the kind of eluent was also investigated in this study. 0.5 M NaCl and SDS-acetic acid (10 % w/v:10 % v/v) were used in the process of elution. The results indicated that SDS-acetic acid (10 % w/v:10 % v/v) has a better elution effect, and with only five elution cycles, template removal was achieved. So we choose it as the eluent in following experiments.

Characterization of magnetic imprinted polymers

The FT-IR spectra of synthesized Fe_3O_4 NPs and Fe_3O_4–MIPs are illustrated in Fig. 2, which provided direct evidences for the synthetic process of Fe_3O_4–MIPs.

The peak at 580 cm^{-1} was attributed to the stretch of Fe-O vibration. the two peaks located at 1560 and 1405 cm^{-1} corresponded to the COO^- anti-symmetrical vibration and COO^- symmetric vibration (Fig. 2A, B), indicating that large amounts of carboxylate groups cover the surface of the Fe_3O_4 through solvothermal polymerization. When compared with Fe_3O_4@COOH, the specific features of Fe_3O_4–MIPs were C–H bond at 2851 and 2922 cm^{-1} (Fig. 2A). These results suggested that APTES and TEOS have been successfully polymerized to form the particles.

The morphological structure and size of Fe_3O_4@COOH and Fe_3O_4–MIPs were characterized by TEM. As can be seen from Fig. 3, the obtained Fe_3O_4 @COOH NPs possessed a spherical structure with a diameter of about 200 nm. And it was found that the as-prepared Fe_3O_4–MIPs with irregular shape contained two or more Fe_3O_4@COOH NPs after imprinting polymerization (Fig. 4), which provide direct proof of successful preparation of Fe_3O_4@COOH NPs embedded MIPs.

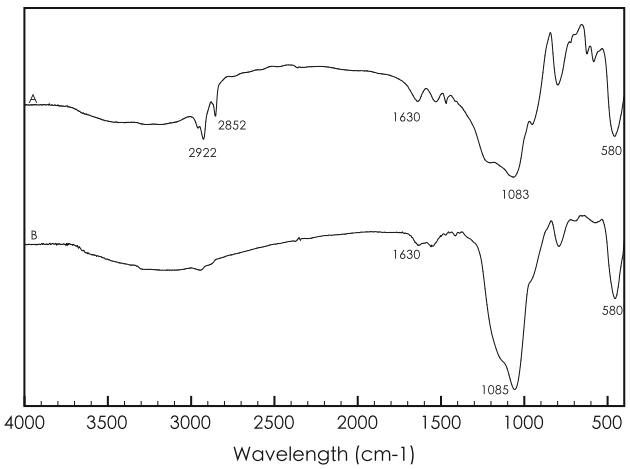

Fig. 2 FT-IR spectra of Fe_3O_4@COOH (*A*) and Fe_3O_4–MIPs (*B*)

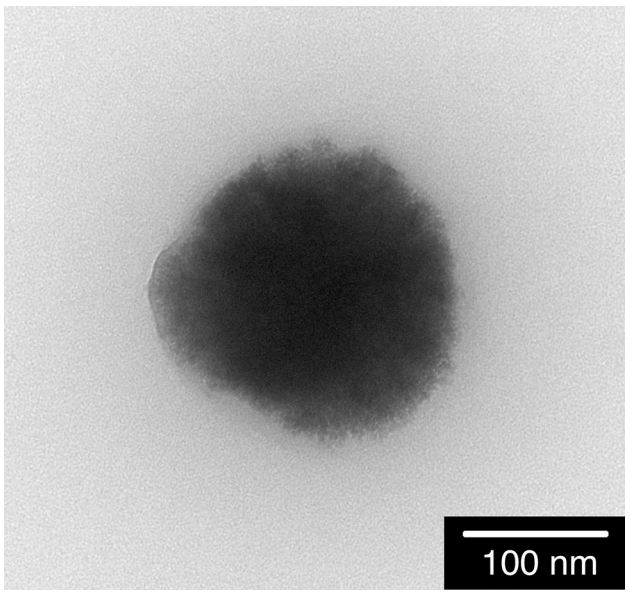

Fig. 3 Transmission electron image of Fe_3O_4@COOH

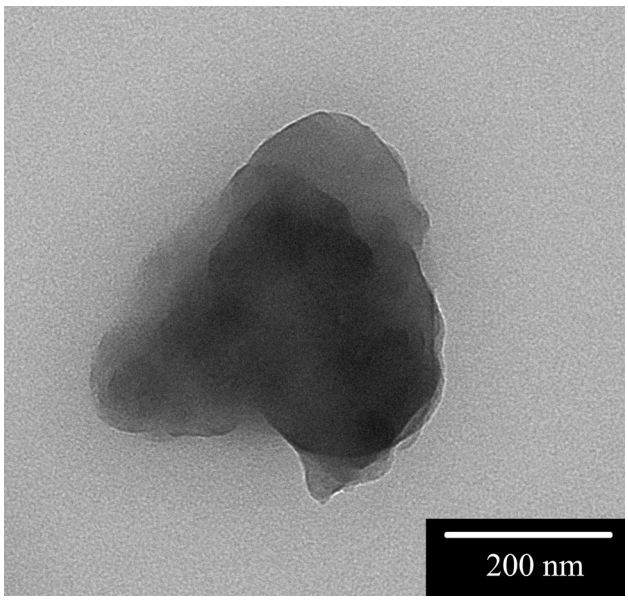

Fig. 4 Transmission electron image of Fe_3O_4–MIPs

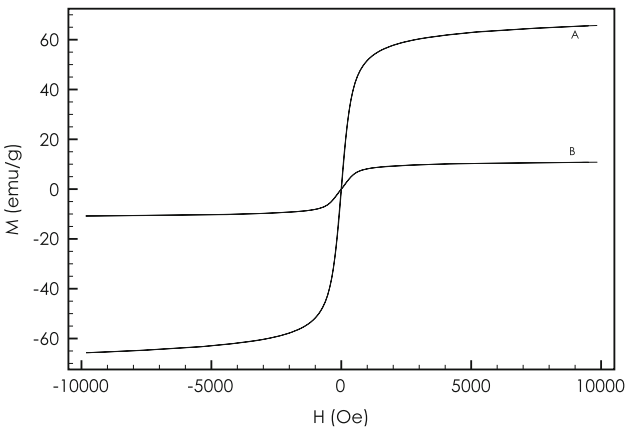

Fig. 5 VSM of Fe_3O_4@COOH (*A*) and Fe_3O_4–MIPs (*B*)

The magnetic properties of the as-prepared Fe_3O_4@COOH NPs and the Fe_3O_4–MIPs were studied by using a VSM at room temperature. Figure 5 illustrates M–H loop of Fe_3O_4@COOH NPs and Fe_3O_4–MIPs. The MH loops show that as-prepared magnetic particles have a fairly strong magnetization and the saturation magnetization values are about 65.70 emu g^{-1} for Fe_3O_4@COOH, which implies a strong magnetic response of the magnetic NPs. The magnetic NPs also show a fast response to the applied magnetic field. After dispersing the Fe_3O_4@COOH NPs in water by shaking, vortexing, or sonication, they can be easily attracted within dozens of seconds by placing a small magnet on the side of the vessel. This suggests that the Fe_3O_4@COOH NPs possess excellent magnetic response and redispersibility, which is very useful for their application. The saturation magnetization values for Fe_3O_4–MIPs was 10.80 emu g^{-1}, lower than Fe_3O_4@COOH. The decrease in magnetic saturation of Fe_3O_4–MIPs may be attributed to the coated imprinting shells on the surface of the magnetic NPs. Notably, from the hysteresis loops it can be seen that there was no remanence and coercivity, which demonstrates that both were superparamagnetic and enable them to be used for separation and enrichment of template proteins.

Binding properties of magnetic imprinted polymers

Binding kinetics

The binding kinetics of Fe_3O_4–MIPs and Fe_3O_4–NIPs were studied (Fig. 6), to reveal the relationship of the binding

capacity of MIPs (NIPs) and the adsorption equilibrium time.

It is clearly shown in Fig. 6 that the binding capacity of MIPs (NIPs) increases at the first 20 min and then an adsorption equilibrium is achieved after 30 min. At the beginning of binding kinetics, a large amount of empty recognition cavities are available in the Fe_3O_4–MIPs, which enable target protein easily to be adsorbed with less resistance. With the growth of time, more and more imprinted cavities were occupied, space steric hindrance became bigger, and the target protein diffused into the empty imprinted cavities became slow. Finally the imprinted cavities were fully occupied, and the adsorption reached equilibrium. Compared with some of previous imprinting work for Lyz binding [26, 28, 31, 46, 47], the adsorption equilibrium time of Fe_3O_4–MIPs for Lyz in this work was short, indicating that good mass transport is got and drawbacks of traditional bulk polymerization is compromised.

Fe_3O_4–NIPs reached a adsorption equilibrium at an very quick speed—just 10 min. But the adsorption capacity is much smaller than that of Fe_3O_4–MIPs. The adsorption amount of Fe_3O_4–MIPs is 8.86 times more than that of Fe_3O_4–NIPs, with the IF for binding Lyz to be 8.86, which is remarkably increased in comparison with previously reported [25] (IF 1.55) and [26] (IF 3.67), and also better than recently reported [47] (IF 7.6) and [46] (IF 8.4).

To further analyze the adsorption kinetics, the pseudo-first-order and second-order kinetic model were applied to fit the kinetic data [50].

The pseudo-first-order kinetic model can be expressed as follows:

$$\ln(Q_e - Q_t) = \ln(Q_e) - k_1 t \quad (4)$$

The pseudo-second-order kinetic model can be expressed as follows:

$$\frac{t}{Q_t} = \frac{1}{k_2 Q_e^2} + \frac{t}{Q_e} = \frac{1}{v_0} + \frac{t}{Q_e} \quad (5)$$

where Q_e and Q_t (mg g^{-1}) are the adsorption capacity and the adsorption amount at the equilibrium and the time t (min), respectively. Q_e(cal) values calculated from the intercept of plot $\ln(Q_e - Q_t)$ versus t, and the slope of t/Q_t versus t are defined as theoretical Q_e(cal) value of pseudo-first-order and pseudo-second-order model, respectively.

k_1 (min^{-1}) and k_2 (mg g^{-1} min^{-1}) are pseudo-first-order and pseudo-second-order rate constants of adsorption, respectively. And v_0 (mg g^{-1} min^{-1}) represents the initial adsorption rate for pseudo-second-order kinetic model.

Pseudo-first-order model is rendered the rate of occupation of the adsorption sites to be proportional to the number of unoccupied sites; pseudo-second-order kinetic model is assumed the chemical reaction mechanisms, and that the adsorption rate is controlled by chemical adsorption through sharing or exchange of electrons between the adsorbrate and adsorbent [50]. Parameters of two kinetic models are given in Table 1. The best-fit model was selected based on both squared linear regression correlation coefficient (r) and the theoretical Q_e(cal) value. For the adsorption of Lyz onto Fe_3O_4–MIPs, the pseudo-second-order rate equation agreed well with the data with $r = 0.99$. And the theoretical Q_e(cal) value were closer to the experimental Q_e(exp). Thus, the adsorption process was a chemical-process. As indicated in Table 1, Lyz adsorption onto Fe_3O_4–NIPs belonged to the pseudo-first-order kinetic model.

As shown in Table 1, the MIPs adsorption data were well fitted by the pseudo-second-order kinetic model, indicating that the rate-limiting step was controlled by chemical adsorption and the adsorption capacity was proportional to the number of active binding sites in MIPs. The NIPs adsorption data were were fitted well by the pseudo-first-order kinetic model.

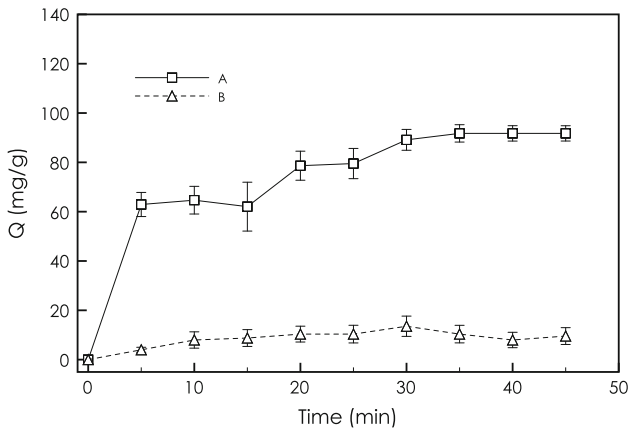

Fig. 6 Binding kinetics of Fe_3O_4–MIPs (*A*) and Fe_3O_4–NIPs (*B*)

Binding isotherms

An adsorption isotherm is a measure of the relationship between the equilibrium concentrations of bound and free template over a certain concentration range and is readily generated from equilibrium batch rebinding studies. The binding isotherms of protein Lyz to Fe_3O_4–MIPs and control Fe_3O_4–NIPs NPs were determined at different initial concentrations and the results are shown in Fig. 7.

It can be seen that the amounts of protein adsorbed onto the imprinted or non-imprinted polymers increased when the concentration of the protein solutions increased. The amount of protein Lyz bound to the Fe_3O_4–MIPs was increased quickly along with the increase of initial protein concentration. And the amount of Lyz bound to Fe_3O_4–

Table 1 Equations and parameters of binding kinetics and isotherms of Fe_3O_4–MIPs and Fe_3O_4–NIPs

Model	Equations and parameters	Fe_3O_4–MIPs	Fe_3O_4–NIPs
First-order kinetics	Equation	$ln(61.8583 - Q_t) = 4.1249 - 0.0605\ t$	$ln(61.8583 - Q_t) = 2.5070 - 0.0611\ t$
	Q_e (mg g^{-1})	61.8583	12.2681
	k_1 (min^{-1})	0.0605	0.0611
	r	0.8852	0.9726
Second-order kinetics	Equation	$t/Q_t = 0.0581 + 0.0101\ t$	$t/Q_t = 0.9478 + 0.0486\ t$
	Q_e (mg g^{-1})	99.4091	20.5953
	k_2	0.0017	0.0025
	v_0 (mg g^{-1} min^{-1})	16.7997	1.0604
	r	0.9694	0.9396
Langmuir isotherm	Equation	$C_e/Q = 0.0049 + 0.0103\ C_e$	$C_e/Q = 0.1952 + 0.1952\ C_e$
	Q_{max} (mg g^{-1})	97.4235	12.0523
	K_L (mL mg^{-1})	2.1146	0.4251
	r	0.9900	0.9432
Freundlich isotherm	Equation	$\log Q = 4.0956 + 0.2325\ logC_e$	$\log Q = 1.2081 + 0.5864\ logC_e$
	K_F (mg g^{-1})	60.0740	3.3472
	m	0.2325	0.5864
	r	0.9644	0.9800

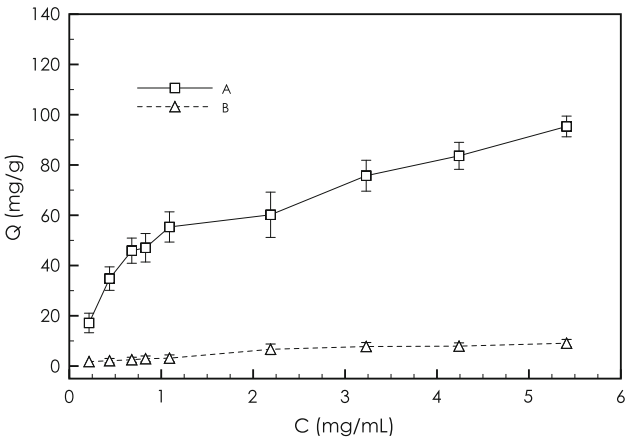

Fig. 7 Binding isotherm of Fe_3O_4–MIPs (*A*) and Fe_3O_4–NIPs (*B*)

MIPs was dramatically higher than that of Fe_3O_4–NIPs at the same initial concentration. The results suggested that the recognition cavities in Fe_3O_4–MIPs had better chemical and steric matching with the template protein. On the contrary, Fe_3O_4–NIPs had no specific binding cavities; thus, the non-specific adsorption was dominant and a lower binding affinity is presented. Therefore, the introduction of Fe_3O_4@COOH for Fe_3O_4–MIPs were expected not only to improve the binding capacity, but also to provide excellent accessibility to target molecules.

Binding properties can be calculated from the binding isotherm by fitting the adsorption isotherm to specific binding models [51]. Langmuir and Freundlich isotherm models are widely used to describe experimental data of binding istherms, which can be respectively expressed as follows:

$$\frac{C_e}{Q} = \frac{1}{Q_{max}K_L} + \frac{C_e}{Q_{max}} \tag{6}$$

$$log\ Q = m\ \log\ C_e + \log\ K_F \tag{7}$$

where Q (mg g^{-1}) is the amount of Lyz bound to Fe_3O_4–MIPs at equilibrium, Q_{max} (mg g^{-1}) is the apparent maximum adsorption capacity, C_e (mg mL^{-1}) is the free analytical concentration at equilibrium, K_L (mL mg^{-1}) is the Langmuir constant related to the affinity of binding sites, K_F (mg g^{-1}) and m are the Freundlich constants which represent the adsorption capacity and heterogeneity of the system. The value of K_L, Q_{max} and m, K_F can be calculated from the slope and intercept of the linear plot in C_e/Q versus C_e and log Q versus log C_e, respectively.

Langmuir isotherm model is basically used for monolayer adsorption onto a surface with a homogeneous system, while Freundlich isotherm model is suitable for multilayer adsorption of heterogeneous system and not restricted to the formation of the monolayer. The results are given in Table 1.

By comparison of r in Table 1, the isotherm models for Fe_3O_4–MIPs and Fe_3O_4–NIPs were better fitted with Langmuir and Freundlich isotherm, respectively. The maximum amount of adsorption (95.3271 mg g^{-1}) obtained from experimental results is also close to the apparent maximum adsorption capacity (99.4091 mg g^{-1})

calculated by Langmuir isotherm model. m value for Fe_3O_4–MIPs and Fe_3O_4–NIPs both were not high. This could be because the as-prepared Fe_3O_4–MIPs and Fe_3O_4–NIPs particles are of irregular form.

The saturation binding data were further processed with the Scatchard equation to estimate the binding properties of the Fe_3O_4–MIPs. The scatchard equation used for this purpose is as follows:

$$\frac{Q_e}{C_e} = \frac{(Q_{max} - Q_e)}{K_d} \quad (8)$$

where Q_e is the amount of Lyz bound to Fe_3O_4–MIPs at equilibrium, Q_{max} is the apparent maximum adsorption capacity, C_e is the free analytical concentration at equilibrium and K_d is the dissociation constant. The values of K_d and Q_{max} could be calculated from the slope and intercept of the linear plot of Q_e/C_e versus Q_e. Scatchard analysis for Fe_3O_4–MIPs was performed and the Scatchard plots were found to be consisted of two distinct linear sections with different slopes (Fig. 8).

This observation indicated that two kinds of binding sites were populated on the imprinted particles. The linear regression equations for the linear regions were $Q_e/C_e = 185.7633 - 2.0141Q_e$ (r = 0.94) and $Q_e/C_e = 54.80531 - 0.37699Q_e$ (r = 0.99). From the slope and the intercept of the straight line obtained, the values of K_d and Q_{max} were 2.014123 mg L^{-1}, 92.23035 mg g^{-1} and 0.3769887 mg L^{-1}, 145.3765 mg g^{-1}, respectively.

With some comparable parameters from literature, further comparisons were made as shown in Table 2, which displays some advantages in aspects of imprinting effects and the presented method in this paper shows an encouraging result.

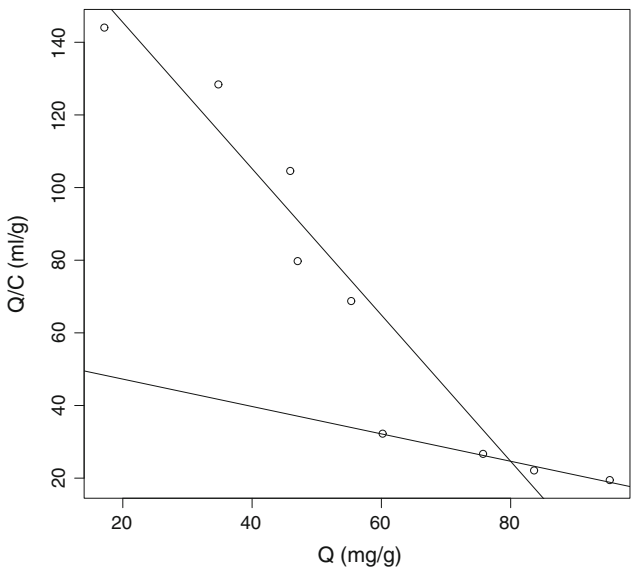

Fig. 8 Scatchard plot of Fe_3O_4–MIPs

Binding selectivity

In order to verify that the Fe_3O_4–MIPs are selective to Lyz (M_W 14.4 kDa, pI 11.2), BSA (M_W 68 kDa, pI 4.7), BHb (M_W 64.5 kDa, pI 7.1) and OVA (M_W 45 kDa, pI 4.6) were selected as the comparative substrates. These proteins have different molecular mass and isoelectric points (pI). The experimental results are shown in Fig. 9 and Table 3, which clearly show that the amount of Lyz adsorbed onto the imprinted Fe_3O_4–MIPs was more than those of the other proteins and 8.86 times more than that of Lyz adsorbed onto the blank Fe_3O_4–NIPs.

The high adsorption ability of the Fe_3O_4–MIPs for the template protein Lyz shows that the differences in the binding amounts stem mainly from specific binding sites on the imprinted cavities. The specific binding involves two roles, including multiple weak interactions provided by the amino (APTES), alkyl (TEOS), and carboxyl (Fe_3O_4@COOH) group and the synergistic effects of shape complementarity. Fe_3O_4–MIPs have not only stronger binding for template proteins but also steric effects hindering comparative proteins from being adsorbed. In the case of BSA and OVA, they are negatively charged at pH 7.0, and both the molecular volumes were larger than that of Lyz, so they had less chance to entirely slip into the imprinting cavities created by Lyz and to interact with the functional groups. As for the BHb, it can be adsorbed onto the surface of Fe_3O_4–MIPs due to their relatively neutral charge at pH 7.0, but imprinted sites on the Fe_3O_4–MIPs are not beneficial for adsorption. The results demonstrated that Fe_3O_4–MIPs have specific recognition sites which are capable of selectively binding Lyz.

Competitive binding test

The binding specificity of Fe_3O_4–MIPs was further evaluated by separating Lyz from standard protein mixtures.

First, binary protein mixture solution with Lyz and BSA were employed for competitive binding (Fig. 10). As seen in Fig. 10, most of BSA remained in the solution but about 40 % of the Lyz were separated after adsorption by the Fe_3O_4–MIPs, while the remaining amount of Lyz and BSA in the protein solution after adsorption by the Fe_3O_4–NIPs was close. It is to say that imprinted cavities are formed successfully and can selectively separate Lyz from a binary mixture of proteins.

Second, ternary protein mixture solution was used for competitive binding test, with Lyz as target protein, BSA and OVA, two types of protein with different molecular weights, as the competitors(Fig. 11). It is seen in Fig. 11 that after Fe_3O_4–MIPs adsorption, more Lyz was separated from the protein solution, BSA was well kept in the protein solution, and OVA was relatively absorbed, while Fe_3O_4–

Table 2 Comparison of protein imprinting with different preparation methods

Target protein	Q_{MIP} (mg g^{-1})	Equilibrium time	IF	Reference
BSA	56.4	150 min	6.51	[1]
BHb	34.51	30 min	4.79	[15]
Hb	281.94	30 min	4.29	[16]
Lyz	5.6	60 min	3.7	[17]
Lyz	202.02	45 min	2.04	[19]
Lyz	17.7	5 min	1.46	[24]
Lyz	39.5	1 h	2.12	[25]
Lyz	c.a. 240	12 h	3.67	[26]
BSA	71.85	120 min	1.70	[27]
BHb	110.5	60–120 min	4.90	[28]
BHb	34.51	6 h	2.07	[31]
Lyz	110	100 min	8.4	[46]
Lyz	104.8	5 h	7.6	[47]
BHb	77.6	150 min	3.1–4.3	[48]
BHb	10.52	1 h	4.6	[49]
Lyz	91.74	30 min	8.86	This paper

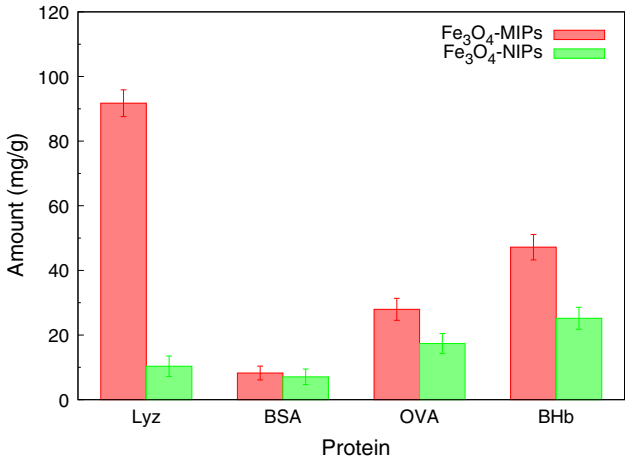

Fig. 9 Binding selectivity of Fe_3O_4–MIPs and Fe_3O_4–NIPs

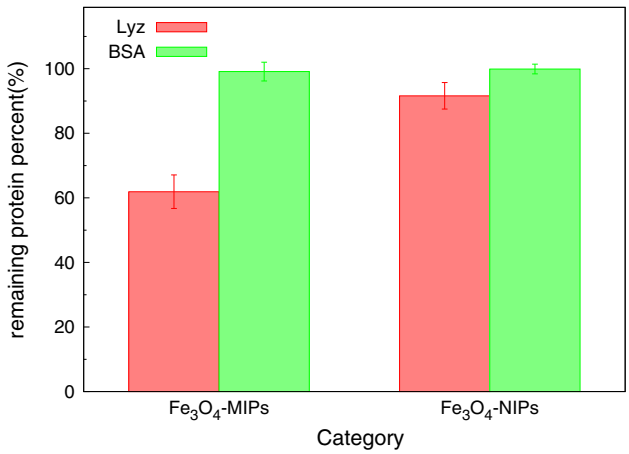

Fig. 10 Competitive binding of Lyz and BSA with Fe_3O_4–MIPs Fe_3O_4–NIPs

Table 3 Binding capacity, imprinting factors, and selectivity coefficients of Lyz, BSA, OVA, and BHb for Fe_3O_4–MIPs and Fe_3O_4–NIPs

Protein	Q_{MIP} (mg g^{-1})	Q_{NIP} (mg g^{-1})	IF	SC
Lyz	91.74	10.35	8.86	–
BSA	8.26	7.08	1.17	7.60
OVA	27.95	17.38	1.61	5.51
BHb	47.20	25.19	1.87	4.73

NIPs absorbed those three proteins with low amounts. The adsorption capacities for the two competing proteins were lower as compared to Lyz mainly due to the steric hindrance. This is a proof of the successful formation of imprinted cavities and the importance of shape memory effect on Fe_3O_4–MIPs. By contrast, the three proteins in mixture solution were slightly adsorbed by Fe_3O_4–NIPs and there was not obvious discrimination among those proteins. Fe_3O_4–NIPs did not have high and selective adsorption ability for three proteins. It was obvious that the Fe_3O_4–MIPs recognized the template Lyz preferentially from a ternary mixture of proteins, which further demonstrated the binding specification.

This result shows that Fe_3O_4–MIPs may be applicable to selectively separate Lyz from a mixture of proteins.

Real sample analysis

To further demonstrate the applicability and separation effectiveness of Fe_3O_4–MIPs in real sample, chicken egg white, in which the concentration of Lyz is about 3.5 %

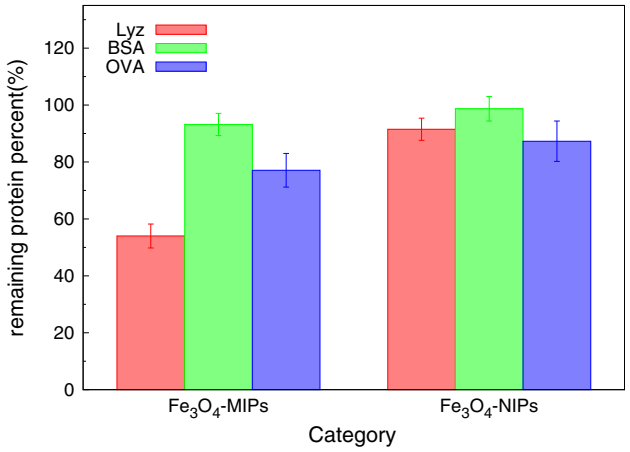

Fig. 11 Competitive binding of Lyz, BSA and OVA with Fe_3O_4–MIPs Fe_3O_4–NIPs

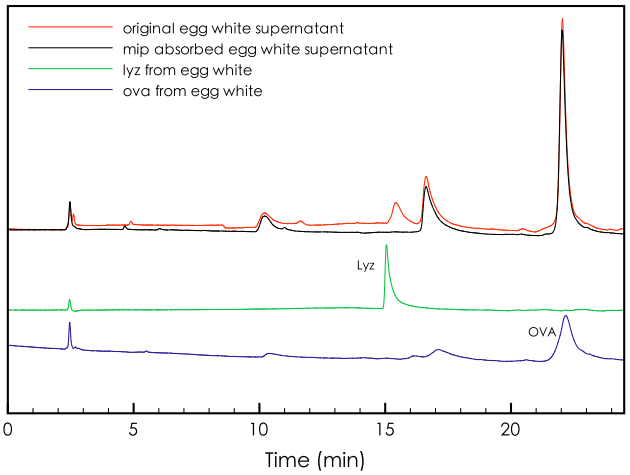

Fig. 13 HPLC analysis of Lyz adsorption with Fe_3O_4–MIPs

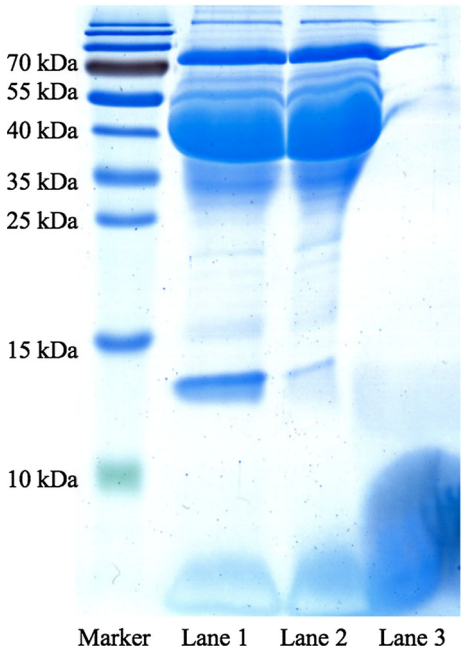

Fig. 12 SDS-PAGE analysis of Lyz adsorption with Fe_3O_4–MIPs

from all proteins was used as a Lyz source [31]. Egg white sample was separated from chicken egg and diluted 20-fold with 1/15 M PB buffer and centrifuged with 10,000 rpm for 20 min. Then Fe_3O_4–MIPs was added into the egg white sample to absorb target protein and later quantification followed.

SDS-PAGE analysis was first employed for real sample test (Fig. 12). It is seen from Fig. 12 that, as compared with original diluted chicken egg white sample (Lane 1), the Lyz was almost completely removed from the chicken egg white sample after absorption by Fe_3O_4–MIPs while the change in other proteins was insignificant (Lane 2). The elution of Lyz also proved the successfully separation (Lane 3).

Next, HPLC was employed for further quantification. The chromatograms of a 20-fold diluted egg white and are shown in Fig. 13. When Lyz in 20-fold diluted egg white was separated by Fe_3O_4@Lyz–MIP using an external magnetic field, the chromatogram of supernatant showed that it (Lyz peak) disappeared, which showed a very good selectivity for target Lyz by Fe_3O_4–MIPs.

As revealed in the real sample competition experiments, the Fe_3O_4–MIPs validated high selectivity toward the template protein, which suggested its potential in practical applications.

Conclusions

Using carboxyl-modified magnetic Fe_3O_4@COOH nanoparticles (NPs) as co-functional monomer and magnetic response source, bulk MIPs were prepared with a sol–gel process for the recognition and enrichment of protein. The as-prepared Fe_3O_4–MIPs showed fast kinetics, high capacity, and favorable selectivity. Successful application in the selective separation of Lyz from standard protein mixture and real egg white sample suggested that the Fe_3O_4–MIPs could be an alternative solution for selectively capturing a protein in a complex matrix.

References

1. Tan CJ, Chua HG, Ker KH, Tong YW (2008) Preparation of bovine serum albumin surface-imprinted submicrometer particles with magnetic susceptibility through core-shell miniemulsion polymerization. Anal Chem 80:683–692

2. Alexander C, Andersson H, Andersson L, Ansell R, Kirsch N, Nicholls I, O'Mahony J, Whitcombe M (2006) Molecular imprinting science and technology: a survey of the literature for the years up to and including 2003. J Mol Recognit 19:106–180
3. Whitcombe MJ, Kirsch N, Nicholls IA (2014) Molecular imprinting science and technology: a survey of the literature for the years 2004–2011. J Mol Recognit 27:297–401
4. Shin MJ, Shin YJ, Hwang SW, Shin JS (2013) Recognizing amino acid chirality with surface-imprinted polymers prepared in W/O emulsions. Int J Polym Sci 2013:1–5
5. Gkementzoglou C, Kotrotsiou O, Kiparissides C (2013) Synthesis of novel composite membranes based on molecularly imprinted polymers for removal of triazine herbicides from water. Ind Eng Chem Res 52:14001–14010
6. Liu J, Yang M, Hou D, Hou C, Li X, Wang G, Feng D (2013) Molecularly imprinted polymers on the surface of silica microspheres via sol-gel method for the selective extraction of Streptomycin in aqueous samples. J Sep Sci 36:1142–1148
7. Xie X, Chen L, Pan X, Wang S (2015) Synthesis of magnetic molecularly imprinted polymers by reversible addition fragmentation chain transfer strategy and its application in the Sudan dyes residue analysis. J Chromatogr A 1405:32–39
8. Xie X, Pan X, Han S, Wang S (2015) Development and characterization of magnetic molecularly imprinted polymers for the selective enrichment of endocrine disrupting chemicals in water and milk samples. Anal Bioanal Chem 407:1735–1744
9. Xie X, Wei F, Chen L, Wang S (2015) Preparation of molecularly imprinted polymers based on magnetic nanoparticles for the selective extraction of protocatechuic acid from plant extracts. J Sep Sci 38:1046–1052
10. Miao S, Wu M, Zuo H, Jiang C, Jin S, Lu Y, Yang H (2015) Core-shell magnetic molecularly imprinted polymers as sorbent for sulfonylurea herbicide residues. J Agric Food Chem 63:3634–3645
11. Zhou Y, Zhou T, Jin H, Jing T, Song B, Zhou Y, Mei S, Lee Y (2015) Rapid and selective extraction of multiple macrolide antibiotics in foodstuff samples based on magnetic molecularly imprinted polymers. Talanta 137:1–10
12. Wang C, Hu X, Guan P, Qian L, Wu D, Li J (2015) Superparamagnetic molecularly imprinting polymers for adsorbent and separation pentapeptides by surface ATRP. Sep Sci Technol 50:1768–1775
13. Ma P, Zhou Z, Yang W, Tang B, Liu H, Xu W, Huang W (2015) Preparation and application of sulfadiazine surface molecularly imprinted polymers with temperature-responsive properties. J Appl Polym Sci 132:41769–41781
14. Chen H, Kong J, Yuan D, Fu G (2014) Synthesis of surface molecularly imprinted nanoparticles for recognition of lysozyme using a metal coordination monomer. Biosens Bioelectron 53:5–11
15. Gao R, Mu X, Hao Y, Zhang L, Zhang J, Tang Y (2014) Combination of surface imprinting and immobilized template techniques to preparation of core-shell molecularly imprinted polymers based on directly amino-modified Fe_3O_4 nanoparticles for specific recognition of bovine hemoglobin. J Mater Chem B 2:1733–1741
16. Liu Y, Gu Y, Li M, Wei Y (2014) Protein imprinting over magnetic nanospheres via a surface grafted polymer for specific capture of hemoglobin. New J Chem 38:6064–6072
17. Li Q, Yang K, Liang Y, Jiang B, Liu J, Zhang L, Liang Z, Zhang Y (2014) Surface protein imprinted core-shell particles for high selective lysozyme recognition prepared by reversible addition-fragmentation chain transfer strategy. ACS Appl Mater Interfaces 6:21954–21960
18. Phan NV, Sussitz HF, Lieberzeit PA (2014) Polymerization parameters influencing the QCM response characteristics of BSA MIP. Biosensors 4:161–171
19. Wan W, Han Q, Zhang X, Xie Y, Sun J, Ding M (2015) Selective enrichment of proteins for MALDI-TOF MS analysis based on molecular imprinting. Chem Commun 51:3541–3544
20. Kameya M, Sakaguchi-Mikami A, Ferri S, Tsugawa W, Sode K (2015) Advancing the development of glycated protein biosensing technology next-generation sensing molecules. J Diabetes Sci Technol 9:183–191
21. Yang Y, He X, Wang Y, Li W, Zhang Y (2014) Epitope imprinted polymer coating CdTe quantum dots for specific recognition and direct fluorescent quantification of the target protein bovine serum albumin. Biosens Bioelectron 54:266–272
22. Yang K, Liu J, Li S, Li Q, Wu Q, Zhou Y, Zhao Q, Deng N, Liang Z, Zhang L, Zhang Y (2014) Epitope imprinted polyethersulfone beads by self-assembly for target protein capture from the plasma proteome. Chem Commun 50:9521–9524
23. Kryscio DR, Peppas NA (2012) Critical review and perspective of macromolecularly imprinted polymers. Acta Biomater 8:461–473
24. He H, Fu G, Wang Y, Chai Z, Jiang Y, Chen Z (2010) Imprinting of protein over silica nanoparticles via surface graft copolymerization using low monomer concentration. Biosens Bioelectron 26:760–765
25. Fu G, He H, Chai Z, Chen H, Kong J, Wang Y, Jiang Y (2011) Enhanced lysozyme imprinting over nanoparticles functionalized with carboxyl groups for noncovalent template sorption. Anal Chem 83:1431–1436
26. Zhang M, Zhang X, He X, Chen L, Zhang Y (2012) A self-assembled polydopamine film on the surface of magnetic nanoparticles for specific capture of protein. Nanoscale 4:3141–3147
27. Li X, Zhang B, Li W, Lei X, Fan X, Tian L, Zhang H, Zhang Q (2014) Preparation and characterization of bovine serum albumin surface-imprinted thermosensitive magnetic polymer microsphere and its application for protein recognition. Biosens Bioelectron 51:261–267
28. Gao R, Kong X, Wang X, He X, Chen L, Zhang Y (2011) Preparation and characterization of uniformly sized molecularly imprinted polymers functionalized with core-shell magnetic nanoparticles for the recognition and enrichment of protein. J Mater Chem 21:17863–17871
29. Li Y, Hong M, Bin Q, Lin Z, Cai Z, Chen G (2013) Novel composites of multifunctional Fe_3O_4@Au nanofibers for highly efficient glycoprotein imprinting. J Mater Chem B 1:1044–1051
30. Herdt AR, Kim BS, Taton TA (2007) Encapsulated magnetic nanoparticles as supports for proteins and recyclable biocatalysts. Bioconj Chem 18:183–189
31. Gai Q, Qu F, Liu Z, Dai R, Zhang Y (2010) Superparamagnetic lysozyme surface-imprinted polymer prepared by atom transfer radical polymerization and its application for protein separation. J Chromatogr A 1217:5035–5042
32. Hua Z, Chen Z, Li Y, Zhao M (2008) Thermosensitive and salt-sensitive molecularly imprinted hydrogel for bovine serum albumin. Langmuir 24:5773–5780
33. Ou S, Wu M, Chou T, Liu C (2004) Polyacrylamide gels with electrostatic functional groups for the molecular imprinting of lysozyme. Anal Chim Acta 504:163–166
34. Odabaşi Say MR, Denizli A (2007) Molecular imprinted particles for lysozyme purification. Mater Sci Eng C 27:90–99
35. Hawkins DM, Stevenson D, Reddy SM (2005) Investigation of protein imprinting in hydrogel-based molecularly imprinted polymers (HydroMIPs). Anal Chim Acta 542:61–65
36. Ghasemzadeh N, Nyberg F, Hjertén S (2008) Highly selective artificial gel antibodies for detection and quantification of biomarkers in clinical samples. I. Spectrophotometric approach to design the calibration curve for the quantification. J Sep Sci 31:3945–3953

37. Ghasemzadeh N, Nyberg F, Hjertén S (2008) Highly selective artificial gel antibodies for detection and quantification of biomarkers in clinical samples. II. Albumin in body fluids of patients with neurological disorders. J Sep Sci 31:3954–3958
38. Chen Z, Hua Z, Xu L, Huang Y, Zhao M, Li Y (2008) Protein-responsive imprinted polymers with specific shrinking and rebinding. J Mol Recognit 21:71–77
39. Lina HY, Hoa MS, Lee MH (2009) Instant formation of molecularly imprinted poly(ethylene-co-vinyl alcohol)/quantum dot composite nanoparticles and their use in one-pot urinalysis. Biosens Bioelectron 25:579–586
40. Lee M, Chen Y, Ho M, Lin H (2010) Optical recognition of salivary proteins by use of molecularly imprinted poly (ethylene-co-vinyl alcohol)/quantum dot composite nanoparticles. Anal Bioanal Chem 397:1457–1466
41. Saridakis E, Khurshid S, Govada L, Phan Q, Hawkins D, Crichlow GV, Lolis E, Reddy SM, Chayen NE (2011) Protein crystallization facilitated by molecularly imprinted polymers. Proc Natl Acad Sci 108:11081–11086
42. Brüggemann O, Haupt K, Ye L, Yilmaz E, Mosbach K (2000) New configurations and applications of molecularly imprinted polymers. J Chromatogr A 889:15–24
43. Sulitzky C, Rückert B, Andrew J, Lanza F, Unger K, Sellergren B (2002) Grafting of molecularly imprinted polymer films on silica supports containing surface-bound free radical initiators. Macromolecules 35:79–91
44. Kempe H, Kempe M (2004) Novel method for the synthesis of molecularly imprinted polymer bead libraries. Macromol Rapid Commun 25:315–320
45. Liu J, Sun Z, Deng Y, Zou Y, Li C, Guo X, Xiong L, Gao Y, Li F, Zhao D (2009) Highly water-dispersible biocompatible magnetite particles with low cytotoxicity stabilized by citrate groups. Angew Chem 121:5989–5993
46. Jing T, Du H, Dai Q, Xia H, Niu J, Hao Q, Mei S, Zhou Y (2010) Magnetic molecularly imprinted nanoparticles for recognition of lysozyme. Biosens Bioelectron 26:301–306
47. Cao J, Zhang X, He X, Chen L, Zhang Y (2014) The synthesis of magnetic lysozyme-imprinted polymers by means of distillation-precipitation polymerization for selective protein enrichment. Chem Asian J 9:526–533
48. Zhang M, Wang Y, Jia X, He M, Xu M, Yang S, Zhang C (2014) The preparation of magnetic molecularly imprinted nanoparticles for the recognition of bovine hemoglobin. Talanta 120:376–385
49. Kan X, Zhao Q, Shao D, Geng Z, Wang Z, Zhu J (2010) Preparation and recognition properties of bovine hemoglobin magnetic molecularly imprinted polymers. J Phys Chem B 114:3999–4004
50. Liu Y, Liu Z, Gao J, Dai J, Han J, Wang Y, Xie J, Yan Y (2011) Selective adsorption behavior of Pb (II) by mesoporous silica SBA-15-supported Pb (II)-imprinted polymer based on surface molecularly imprinting technique. J Hazard Mater 186:197–205
51. Umpleby R, Baxter S, Chen Y, Shah R, Shimizu K (2001) Characterization of molecularly imprinted polymers with the Langmuir-Freundlich isotherm. Anal Chem 73:4584–4591